Predicting S4 Beam Joint Nonlinearity using Quasi-Static Modal Analysis

Mitchell Wall, Matthew S. Allen and Iman Zare

Department of Engineering Physics
University of Wisconsin-Madison
1500 Engineering Dr. Madison, WI 53706

ABSTRACT
Recently, a new algorithm was presented [Festjens et al., Int J Mech Sci 75 (2013) 170–177] that allows one to predict the effective natural frequency and damping ratio as a function of amplitude for a structure with bolted joints. This paper applies a variant on that algorithm to a finite element model of the "S4 Beam" (two C-shaped beams bolted together on their ends) and compares the results with the measurements described in [Singh et al., IMAC 2019]. The algorithm, which is here referred to as Quasi-Static Modal Analysis (QSMA), is applied to a detailed finite element model of the beam in the commercial software package, Abaqus®. Coulomb friction is assumed to govern the contact interface. Amplitude dependent damping and natural frequency curves are calculated for the structure and compared to experimental measurement. Several studies are included which explore the solver tolerances and preload values needed to reach agreement with experimental measurements. Additionally, the shape of the actual contact interfaces is measured using a profilometer and fed into the model to quantify the effect of slight curvature in the contact.

Keywords: Quasi-Static Modal Analysis, Nonlinearity, FEA, Damping, Natural Frequency

1. INTRODUCTION

The dynamic response of large structures is determined by their inertia, stiffness and damping properties. While mass and stiffness properties can be readily deduced from design data, the prediction of damping properties is difficult, particularly in the case of nonlinear damping caused by friction in joints. Although mechanical joints are integral parts of most engineering structures, their effects on structural dynamics are not yet fully understood. Frequently, our ability to design dynamically loaded structures is hampered by the linear and nonlinear behavior of joints; because the joints aren't well understood, they are represented using simplified elements whose parameters must be identified or tuned through testing. As pointed out by Berger [1], joints are governed by physics at a length scale orders of magnitude smaller than the structures, so analysts are faced with a trade-off in the spatial resolution of the nonlinear degrees of freedom within a joint interface versus the computational effort required to evaluate such a model.

Although bolted joints are needed in almost all structures, they are a large source of uncertainty in the stiffness of the structure, and that stiffness is typically weakly nonlinear due to the joints. Furthermore, dissipation due to frictional slip in joints typically far exceeds the material damping, and the damping tends to nonlinear, increasing by a factor of 2-10 at high vibration amplitudes. Energy dissipation helps to reduce vibration amplitudes and decreases the loads on a structure. Hence, any predictions of the life of a structure may be erroneous if this effect is not taken into account in the design phase. If a more accurate estimate of a structure's capacity for energy dissipation can be computed for different levels of environment loading, then engineers can be better informed so as to create more lightweight designs for aircraft and spacecraft, and perhaps even design joints to exploit this effect to maximize dissipation.

The energy dissipation in joints comes about due to the slip in the contacts between components. In each cycle of vibration, the loads on the joints cause some regions within the contact to slip relative to each other while other regions remain stuck [2]. Depending on the transmitted load, the contact interface is divided into stick and slip zones. Bolted joints exhibit two types of motion during vibration, micro-slip, in which only the outer edges of the contact region experience slip, and macro slip, in which the entire joint experiences slip [3].

In analyzing the dynamic response of structures, it is common to represent the friction that occurs at contact surfaces by means of Coulomb friction law. As simple Coulomb models with few parameters oversimplify the description of frictional joints, a continuous model with the ability to include micro-slip seems to be advantageous. Moreover, we should consider that the coefficient of friction is also not constant. It depends primarily on the contact surface properties which change during slip, and on the magnitude of the clamping pressure exerted by the bolts. In [4], it is shown that the coefficient of friction decreases with increasing clamping pressure. According to [5], for "practical surfaces" the coefficient of friction decreases approximately linearly with an increasing normal load.

In order to represent micro-slip friction accurately, the finite element model typically requires a mesh of elements having far greater density in the region of the joint compared to the rest of the structure. Computationally, high-fidelity models may be feasible for simple structures that contain one or a few joints, though some simplifications may be employed to speed up the computational time such as model-order reduction of the linear domain away from the joint. Using the best of these approaches, the time required to simulate the response to a dynamic loading is still on the order of hours, and this time would stretch to weeks or months for more realistic structures, such as the turbofan jet engine, which can contain hundreds of bolted joint interfaces.

It can be claimed that when a structure vibrates in the shape of one of its modes, the joints dissipate energy and lose stiffness in a manner that is unique to that mode. When the structure is excited to higher response amplitudes, the loss in stiffness and increase in energy dissipation can be observed experimentally as a decrease in the natural frequency and increase in the damping ratio, respectively, for that mode. Both the natural frequency and the damping can be retrieved for each mode using well-established experimental practices and signal processing techniques. The current techniques for extracting the frequency and damping from a model are based on signal processing of the simulated response. Both the signal processing techniques and dynamic simulations are prohibitively expensive to compute, which devalues their use in a practical model updating routine.

The problem of computational expense in dynamic simulations was overcome by treating the joint as a quasi-static subcomponent in an otherwise linear, dynamic global model. The groundwork for this solution was laid out in a paper by Festjens et al. [6]. They used the fact that the contact nonlinearity is governed by micro and meso-scale parameters (geometry, roughness, local pressure, etc.) and as a result cannot be included in a macro-size model of a whole structure because of the computational cost. They investigate the idea of using the normal modes of the linearized structure as boundary conditions on a detailed model reduced to the joints only. It has been observed that after a number of repetitive loading cycles, the response of a bolted joint structure may lead to a stabilized state called limit cycle and in the case of an assumed linear structure, this limit cycle is known [6]. Moreover, we can consider the fact that under linear assumption the use of modal coordinates is useful to reduce the size of vibrational problems [7], [8].

After a few modifications to the approach of Festjen et al [6], Allen et al. [9] later presented a fast and efficient computational method for extracting the amplitude-dependent modal properties from a finite element model and applied it to structures where the joints were modeled as discrete Iwan elements. The new method termed "quasi-static modal analysis" (QSMA), estimates the effective modal natural frequency and damping from a single, static deflection in response to a monotonically-increasing load distributed over the entire structure in the shape of one of its modes. Masing's rules are then applied to the force-deflection relationship to quantify the amount of energy dissipated and stiffness lost in the all joints when the structure vibrates in the mode of interest [9]. For Allen et al.'s work, Iwan elements were selected since they can capture microslip efficiently, which gives rise to energy dissipation and nonlinear behavior of the joint. However, Iwan elements require four parameter inputs that must be tuned based upon prototype results since they cannot be deduced from first principles but must be measured experimentally [10], [11].

The method of QSMA dramatically reduces the computational effort because the change in the natural frequency and damping of each mode with modal amplitude can be completely determined from a single set of quasi-static, monotonic loading cases. This is in stark contrast to a dynamic simulation, where the free-response history must be computed until its amplitude decays to the smallest level of interest [12]. This advancement prompted Jewell, Allen & Lacayo [13] to apply this technique to detailed finite element models that included nonlinear contact between the bolted interfaces using a commercial software package. While their results showed that such an analysis is feasible, they struggled to obtain accurate results and noted that, once the structure had been meshed with adequate fidelity to capture micro-slip, the computational cost was very significant even to perform a single static analysis.

Zare and Allen [14], [15] explored a more computationally efficient alternative that follows the work of Ahn and Barber [16], [17] in that they combined QSMA with a static reduction technique, retaining only those DOF on the interface. They implemented the QSMA for structures where the joint is modeled in detail, using a block Gauss-Seidel algorithm to solve the nonlinear contact problem in Matlab.

In this paper, a model of the S4 Beam is constructed in the commercial finite element analysis software package, Abaqus®, with a Coulomb friction law assigned at the interfaces between the parts. The model is loaded using Quasi-Static Modal analysis, and the nonlinear frequency and damping behavior is predicted and compared to experimentally measured properties for a single mode. Several parameters are studied in order to create an efficient and accurate model, such as, convergence tolerances, preload, and small perturbations in the flatness of the surface.

2. BACKGROUND

The Quasi-Static Modal Analysis method implemented in this paper is similar to one developed by Festjens, Chevallier, and Dion, [6], where the effective natural frequency and modal damping ratios are extracted from a nonlinear static analysis. This is done by imposing a quasi-static load to the model that would excite only a single mode of the linearized structure. Allen and Lacayo, [12] recently elaborated on this method, and used the modal load-displacement curves to construct a hysteresis curve from which the effective natural frequency and damping were estimated. The method is reviewed below.

Suppose that a preload is applied to a structure such that the members come into contact in at least one location. The equation of motion for the coupled structure(s) can then be written as

$$\mathbf{M}\ddot{\mathbf{x}} + \mathbf{C}\dot{\mathbf{x}} + \mathbf{K}\mathbf{x} + \mathbf{f}_J(\mathbf{x}, \boldsymbol{\theta}) = \mathbf{f}_{ext}(t) \tag{1}$$

where **M**, **C**, and **K** are, respectively, the mass, damping, and stiffness matrices of the system, and $\mathbf{x}$, $\dot{\mathbf{x}}$, and $\ddot{\mathbf{x}}$ are the displacement, velocity, and acceleration vectors, respectively. The vector $\mathbf{f}_J$ represents the internal forces due to a joint model containing internal sliders, and $\boldsymbol{\theta}$ is a vector that captures the state (slip or stick) of each slider element.

At low vibration amplitudes, the joints can be replaced with springs equivalent to the preloaded stiffness of the joints (when vibratory loads are small),

$$\mathbf{K}_T = \left.\frac{\partial \mathbf{f}_J}{\partial \mathbf{x}}\right|_{\mathbf{x}=\mathbf{0}} \tag{2}$$

where $\mathbf{x} = 0$ corresponds to the preloaded state and an eigenvalue problem can be solved to estimate the mass-normalized mode shapes, φ_r, of the structure.

$$([\mathbf{K} + \mathbf{K_T}] - \lambda \mathbf{M})\varphi_r = 0 \tag{3}$$

At this point, Festjens et al. [6] divided Eq. (1) into a nonlinear domain near the joint and a linear domain away from the joint. While their approach could reduce the computational burden, it does require a specialized implementation and introduces additional uncertainties as there is an additional convergence tolerance governing the connection between the linear and nonlinear domains. Allen and Lacayo instead let the nonlinear domain encompass the entire structure, in which case only one nonlinear static analysis is needed per mode. Using their approach [9], the following quasi-static problem is solved.

$$\mathbf{K}\mathbf{x} + \mathbf{f}_J(\mathbf{x}, \boldsymbol{\theta}) = \mathbf{M}\boldsymbol{\varphi}_r \alpha \tag{5}$$

where α is a scalar which sets the load amplitude. A finite element package returns the response, $\mathbf{x}(\alpha)$, which can then be mapped onto the *r*th mode using:

$$q_r(\alpha) = \boldsymbol{\varphi}_r{}^{\mathrm{T}} \mathbf{M}\mathbf{x}(\alpha) \tag{6}$$

Then using Masing's rules, the force (and similarly displacement) over a full loading cycle can be estimated yielding the following forward and reverse curves. To avoid the computing of a complete cycle for each energy E, it is assumed that the hysteretic behaviors of the joint follow the Masing rules [18]. This description simplifies the modeling of hysteretic behaviors if a full cycle in a force-amplitude hysteresis can be extrapolated from the initial loading (so-called backbone curve) [6].

$$\begin{aligned} \hat{f}_1(q_r) &= 2 f_r\left(\tfrac{q_r + q_r(\alpha)}{2}\right) - \alpha \\ \hat{f}_2(q_r) &= \alpha - 2 f_r\left(\tfrac{q_r(\alpha) - q_r}{2}\right) \end{aligned} \tag{7}$$

The secant of this hysteresis curve is then used to estimate the instantaneous natural frequency of the mode in question:

$$\omega_r(\alpha) = \sqrt{\frac{\alpha}{q_r(\alpha)}} \tag{8}$$

The energy dissipated for each vibration cycle is the area under the hysteresis curve,

$$\begin{aligned} D_r(\alpha) &= \int_{-q_r(\alpha)}^{q_r(\alpha)} \left(\hat{f}_1(q_r) - \hat{f}_2(q_r)\right) dq_r \\ &= 2\int_{-q_r(\alpha)}^{q_r(\alpha)} \left(f_r\left(\tfrac{q_r + q_r(\alpha)}{2}\right) + f_r\left(\tfrac{q_r(\alpha) - q_r}{2}\right) - \alpha\right) dq_r \end{aligned} \tag{9}$$

The integral above is readily evaluated using the trapezoid rule and then the effective damping ratio $\zeta_r(\alpha)$ may be determined by analogy with a linear system [9], [12].

$$\zeta_r(\alpha) = \frac{D(\alpha)}{2\pi\left(q_r(\alpha)\omega_r(\alpha)\right)^2} \tag{10}$$

3. MODEL CREATION

The structure of interest was named the S4 Beam in [19] and is shown in Figure 1. The structure consists of two C shaped beams, bolted together at each end. Impact testing was used to determine the amplitude dependent natural frequency and damping for the first several modes of the structure. These experimental measurements will be compared with the amplitude dependent natural frequency and damping predicted from various finite element models. A detailed explanation of experimental setup for the S4 Beam can be found in [19].

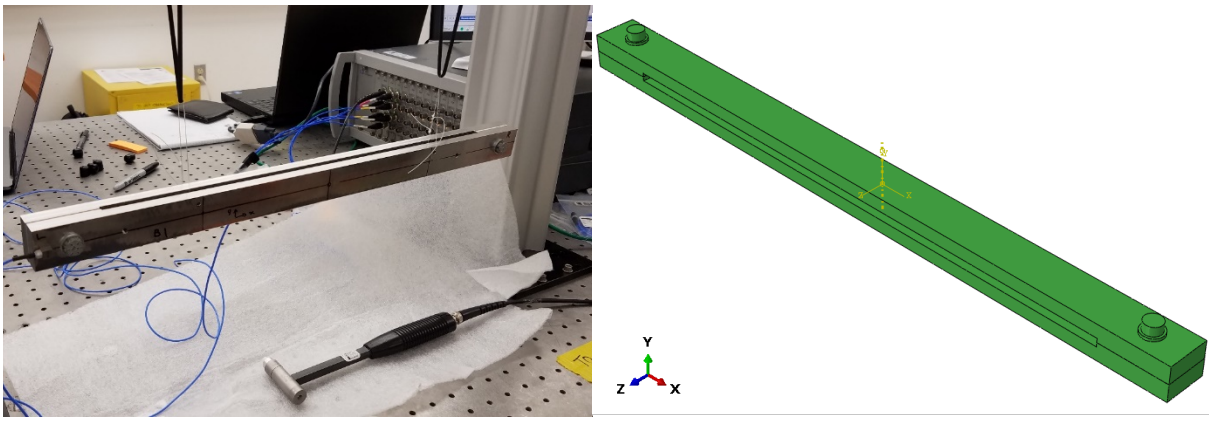

Figure 1: (left) Photo of a test on the S4 Beam. (right) S4 Beam finite element model.

The finite element model used in this work borrowed from the 3D model created in [20], using the parameters, mesh density, etc. previously found to give reasonable results. For the S4 Beam, the mesh density very close to the hole (where slip does not occur until very large loads), as well as along the long beam section was coarsened to reduce computational cost. Tangential contact behavior was defined using the penalty method and μ = 0.6. Normal behavior was also defined with the penalty method with "Hard" contact defined as the pressure-overclosure parameter and a contact stiffness scale factor of 10. The tangential penalty constraint was set to 10^{-6}, which is much tighter than the default, as was found to be necessary in [20]. The model consists of 386,666 user defined nodes and 348,818 user defined elements. All models with reported solve times were solved on a computer with 16 Gb of memory allocated to the solution (of 32Gb) and a 3.6 GHz, Intel® i7-7700 processor using 2 cores (of the 8 available; Windows® treats the four physical cores as 8). The time to solve on two cores was only about 5-10% less than the time required to solve on a single core, so additional parallelization was not explored.

The simulation was split into two steps. First, the preload was applied in a nonlinear loading step in Abaqus and the modes shapes were found using a linear modal analysis. Inertial relief was applied so that preload analysis could be performed on this free-free model. The inertia relief process was apparently not perfect, so an additional rotational constraint was applied to the center of the beams during the preload process. The nodes in contact were then welded together (according to Abaqus's default practice) for the modal analysis. Then the quasi static modal force was calculated in Matlab® as described in Eq. (5) and applied to the structure. The amplitude of the deflection will be referred to in units of thicknesses of the beam (i.e. in some models, the beam was deflected to 0.01 thicknesses of the beam). Inertial relief was also applied in the quasi static loading step, but in this step no additional constraints were needed.

3.1 BOLT PRELOAD

Bolt preload was an important parameter to experiment with because it has a high level of uncertainty. In some cases, the preload of the bolt can vary +/-35% for a given torque level [21]. For the 5/16 x 24 grade 8 bolts used in the actual experiment, one can calculate the nominal preload force using a torque-tension relationship. In this case the Motosh equation 11 was used [22].

$$T = F\left(\frac{P}{2\pi} + \frac{\mu_r r_t}{\cos(\beta)} + \mu_n r_n\right) \tag{11}$$

Here in Eq. (11), the torque applied to the bolt, T, is related to the preload force, F, and multiplied by three terms. The first accounts for the load transferred due to the pitch of the threads, P. The second term is the frictional loss incurred in the threads, where μ_r is the coefficient of friction between the threads on the bolt and the nut, r_t is the effective diameter of the threads, and β is the half angle of the threads. The last term is the friction loss incurred between the head of the bolt and the clamped member, where μ_n is the coefficient of friction between the head and the clamped member and r_n is the effective diameter of the bolt head contact region. For the purposes of these calculations, a coefficient of friction of 0.1 was used for both the threads and head of the bolt, though these numbers can vary widely. A load of 21.2 Kn. is calculated after using data

from [23] to estimate the effective diameter of the threads and bolt head contact region. This load will be varied to quantify its effect on the amplitude dependent natural frequency and damping of the S4 Beam model.

3.2 MODELING SURFACE CURVATURE

The joint interfaces on the beams were machined to be nominally flat, but measurements revealed that there was some curvature, and so an effort was made to quantify the curvature of the contact patches and apply this to the FEM. In later sections of this paper, the measured surface contours of the beams were applied to the nodal positions on the joint interface to model a more realistic contact. In order to do this, surface contour plots were constructed which showed that the nominally flat surfaces had variation of up to 150 μm in height. Two measurements were used to extrapolate a surface contour. Referring to the coordinate system in Figure 1, one measurement was parallel with the X axis and one with the Y, both measurements intersecting at the center of the bolt hole. Each measurement was fit with a 6^{th} degree polynomial. All fits had R^2 values of greater than 0.97. The curvatures in *x*- and *y*- were then added together to approximate the surface of the real machined components. For brevity, the measurements and the fits to them were not included here, but plots of the surface profiles are shown in Figure 2. The titles above each surface indicate which interface they belong to, referring to the coordinate system in Figure 1. For example, the +Y, +X surface is on the top beam on the right joint in Figure 1, and -Y, -X would be on the bottom beam on the left.

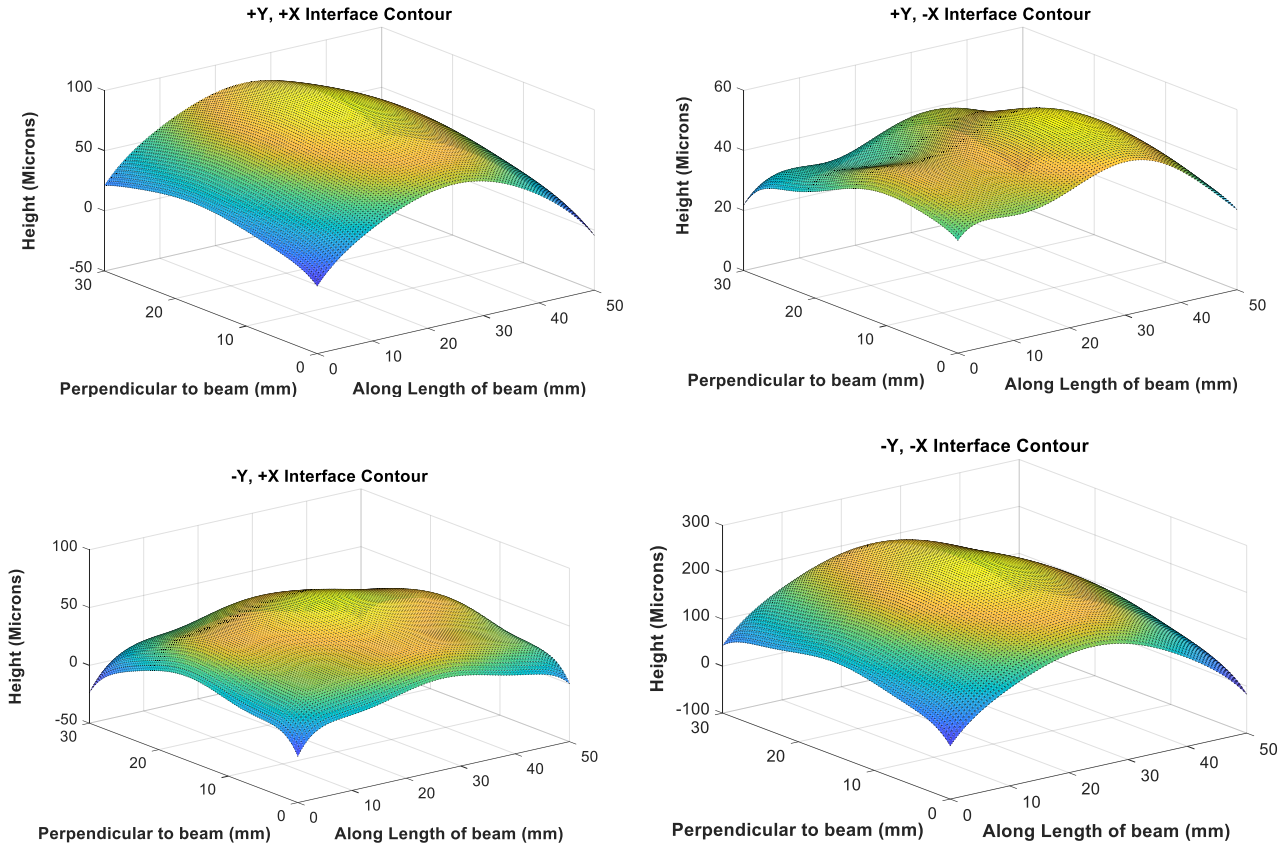

Figure 2: Polynomial fit to surface shapes for the S4 Beam. Four surfaces were fit, two on each end of the beam. The bolt hole, which is not shown in these fits, would be at the center of each of the surfaces shown.

It should be clearly stated that the surface contours for this model are gross approximations meant only to roughly represent the variations in the surfaces. This method is likely a poor approximation of the edges of the interfaces, but as is shown later, the edges of the interface likely play no role in the contact of the joint.

4. TEST CASES

In seeking to obtain agreement between the simulations and the experimental measurements, three main variables were studied. The solver tolerances were varied to find the settings that provide the minimum solve time without sacrificing significant accuracy. The preload of the bolt was varied over multiples of the nominal value to span any uncertainty in the actual load. And finally, the measured surface contour was applied to the interfaces of the FEM to quantify the effect of small but realistic changes to the interface geometry on the results. In all models, mode 2 of the S4 Beam was used. Figure 3 shows that mode 2 is first order, in phase bending mode with motion in the Y-direction.

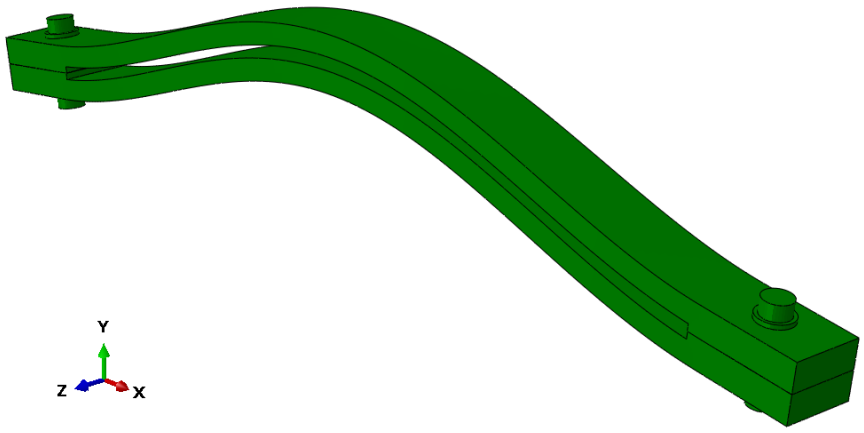

Figure 3: Mode 2 of the S4 Beam.

4.1 SOLVER TOLERANCES

When initially creating many of the models in this paper, convergence issues caused the models to take several days to solve and many did not converge at all. Computation time was also a topic of discussion in [20], which was a precursor to this work. Hence, the solver settings were explored further to seek to speed up the computations. The default solution control parameters defined in Abaqus/Standard are designed to provide reasonably optimal solution of complex problems involving combinations of nonlinearities as well as efficient solution of simpler nonlinear cases. However, the most important consideration in the choice of the control parameters is that any solution accepted as "converged" is a close approximation to the exact solution of the nonlinear equations. We can reset many solution control parameters related to the tolerances used for field equations. If we define less strict convergence criteria, results may be accepted as converged when they are still close to the exact solution of the system but with the less computational cost. In this research, we've changed two parameters to get the accurate results in the acceptable amount of time, C_n^α and R_n^α. Most nonlinear engineering calculations will be sufficiently accurate if the error in the residuals is less than ($\frac{1}{2}$%). Therefore, Abaqus/Standard normally uses:

$$r_{max}^{\alpha} \leq R_n^{\alpha} \overline{q^{\alpha}} \tag{12}$$

where r_{max}^{α} is the largest residual in the balance equation for field α and $\overline{q^{\alpha}}$ is the instantaneous magnitude of the force for field α at time t, averaged over the entire model.

If this inequality is satisfied, convergence is accepted if the largest correction to the solution, C^{α}_{max} , is also small compared to the largest incremental change in the corresponding solution variable Δu^{α}_{max},

$$C^{\alpha}_{max} \leq C^{\alpha}_{n} \Delta u^{\alpha}_{max} \tag{13}$$

where C^{α}_{max} is the largest correction to any nodal variable of type of α provided by the current Newton iteration.

The defaults are $5\text{x}10^{-3}$ for R^{α}_{n} and $2\text{x}10^{-2}$ for C^{α}_{n}. Table 1 presents the results of a study in which, the convergence tolerances were varied and the corresponding solve times are listed. The solve time is given in what Abaqus defines as "wall clock time", or the total time from the submission of the job to the completion.

-	C^{α}_{n}				
R^{α}_{n}	-	$2\text{x}10^{-2}$	$2\text{x}10^{-1}$	$2\text{x}10^{0}$	$2\text{x}10^{1}$
	$5\text{x}10^{-3}$	N/A	N/A	N/A	-
	$5\text{x}10^{-2}$	10.59	12.57	10.96	-
	$5\text{x}10^{-1}$	5.82	5.07	5.60	-
	$5\text{x}10^{0}$	-	-	-	5.77

Table 1: Solve time (hours) and convergence tolerances for the 0.02 thickness deflection models. N/A signifies models that did not solve after 2+ days.

The solve time was improved drastically by increasing R^{α}_{n}. Up until 100 times the default value the solve time decreased. Furthermore, while the results of these computations are not shown here for brevity, each of these solutions gave damping curves that differed by less than 0.001% after the results were processed with QSMA. Since R^{α}_{n} governs the largest residual in the model, it appears that, if the value is set too low, the solver spends a lot of time iterating between solutions when it is already very close to being converged. Relaxing this tolerance still gives good results while also decreasing the solve time drastically. To obtain the maximum speed while keeping the tolerance as small as possible, $R^{\alpha}_{n} = 5\text{x}10^{-1}$, or 100x the default, was used for many of the subsequent models in this paper.

4.2 BOLT PRELOAD

In the experimental measurements presented in [19], the only parameter measured to estimate the preload of the bolt was the torque applied. Given the possible variation in the coefficient of friction as well as the nonlinear dependence of coefficient of friction with pressure [4], a large uncertainty is assumed in the experimental bolt preload. The max tensile strength of a grade 8, 5/16" x 24 bolt is about 31.1 kN loads up to 84.4 kN were tested in order to span all possible loads and then exceeding the possible loads to show the level of preload needed to obtain correlation with experimental results. In total, factors of 0.5x, 1.5x, 2x and 4x were applied to the nominal bolt preload of 21.2 kN calculated in section 3. The general trend is that as the preload increases the structures natural frequency is increased and the damping is decreased.

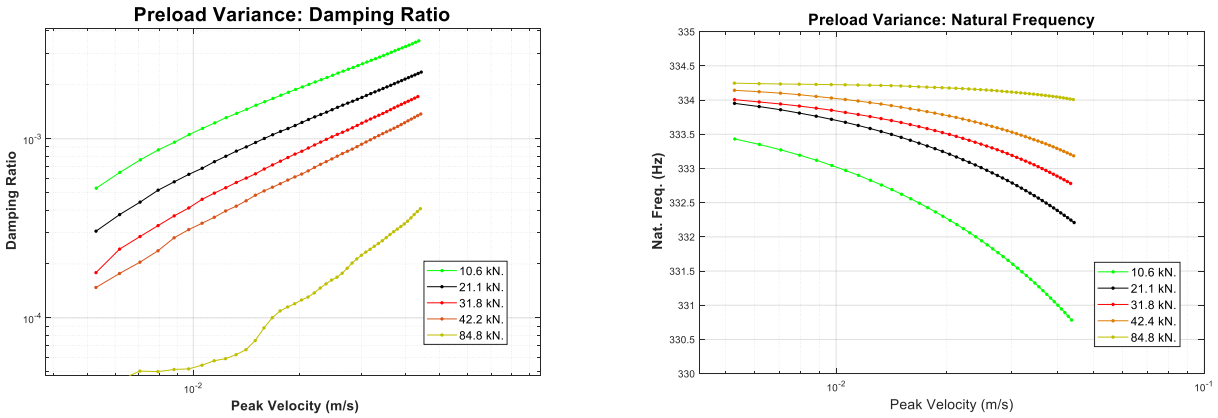

Figure 4: Variation in Effective Damping Ratio and Natural Frequency with Preload

It is also worth noting that the preload in the joint, and thus the amount of microslip occurring, had a substantial effect on solve time. For all the load cases within the physical limitation of the bolt, the solve time decreases with preload, likely because of reduced slip and hence the reduced computational cost of modeling slip. Though once very high loads were reached, computational costs increased rapidly. Solve times for the preceding models are shown in Table 2: Solve time vs. preload. The solve times are from models with $R_n^\alpha = 5X10^{-2}$ and $C_n^\alpha = 2X10^{-1}$.

Preload (kN.)	Solve Times (Hours, Abaqus Wall Clock Time)
42.4	21.8
31.8	7.46
21.2 (nominal)	9.97
10.6	18.92

Table 2: Solve time vs. preload.

These results are not presented for the purpose to showing which model is most efficient, but only to show that there are other factors that may slow down or speed up the simulation depending on the preload in the model. At the moment, the exact causes of the spike in computational cost at very high preloads are unclear, but it is likely that the high preload is causing some nodes to jump in and out of contact, and the solver tolerances may be too strict to address this in an efficient manner.

Figure 5 compares the damping from these simulations with the measured damping. When damping values are compared to experimental data, extremely high preloads are needed to bring the model near agreement with the experimental damping measurements. The cyan curve shows the raw experimental data, and the subsequent curves account for the lack of material, and any other form of linear damping in the FEM by subtracting a constant value from the experimental curve. Values of $\zeta = 0.0004$, $\zeta = 0.0006$ and $\zeta = 0.0008$ are shown to span reasonable values for damping in the linear regime, although the curve using, $\zeta = 0.0006$ produces damping from the joint that most closely obeys a power-law model [24] and is thought to be the most reliable curve.

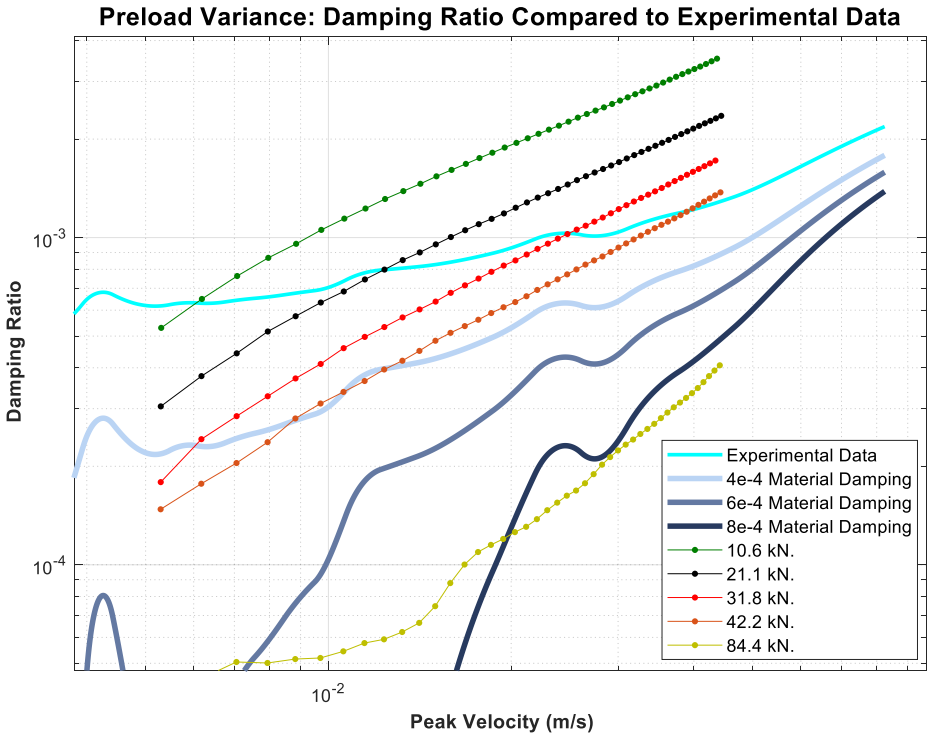

Figure 5: Preload variance and experimental data with various values of material damping.

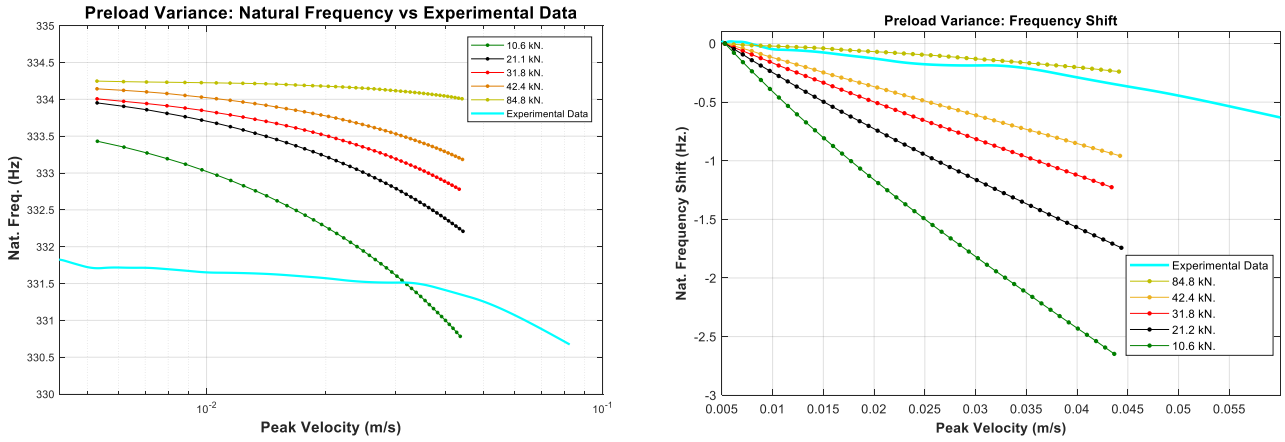

Figure 6: (left) Preload variance and experimental natural frequency curves, (right) frequency shift for preload variance models and experimental data.

When frequency shift is plotted in Figure 6, it is clear that the 84.8 kN model agrees with the experimental data the best. But, the frequency shift is very small so all models show reasonably good agreement with experimental measurements, always being less than 1% away from the measured values.

The results in Figure 6(left) show that the linear natural frequency predicted by the model is 0.9% higher than the measured value. In [19], additional correlation was performed to reach agreement in the experimental modes of one half of the S4 Beam and a FEM. The elastic modulus needed to be shifted -6.05% in order to bring the FEM into agreement, which may explain why some discrepancy in the experimental measurements and the FEM presented here. The effect of the contact on the linear natural frequencies was studied in detail in [23] and so was not investigated further here.

In summary, this preload study shows that the model does show promise in predicting the nonlinear stiffness and damping of this structure, as the simulations and experiments agree in a qualitative sense and are not so far off quantitatively. However, it is not possible to bring both natural frequency and damping ratio into agreement without an impossibly high preload on the bolt, so clearly there are unmodeled physics that must be addressed.

4.3 SURFACE CONTOURS

To explore the issues previously stated, efforts were made to model the geometry of the contact more precisely. Efforts were made in [19] to use profilometry to measure the actual roughness and topography of the surface. While the measurements were not completely successful (the sample was too large for the machine used), sizeable variation in the surface shape was discovered. As described in Section 3, these measurements were used to estimate the profile of the surface and this was applied to the FEM by moving the nodes in the contact surface. The models were then solved as described previously under various preloads. First, the contact patch will be examined. The CSTATUS output from Abaqus is shown in Figure 7. This shows the regions in the model that are either stuck, slipping or not in contact. On the left is the contact patch for the flat FEM interface and on the right is the contact patch for the modified interface.

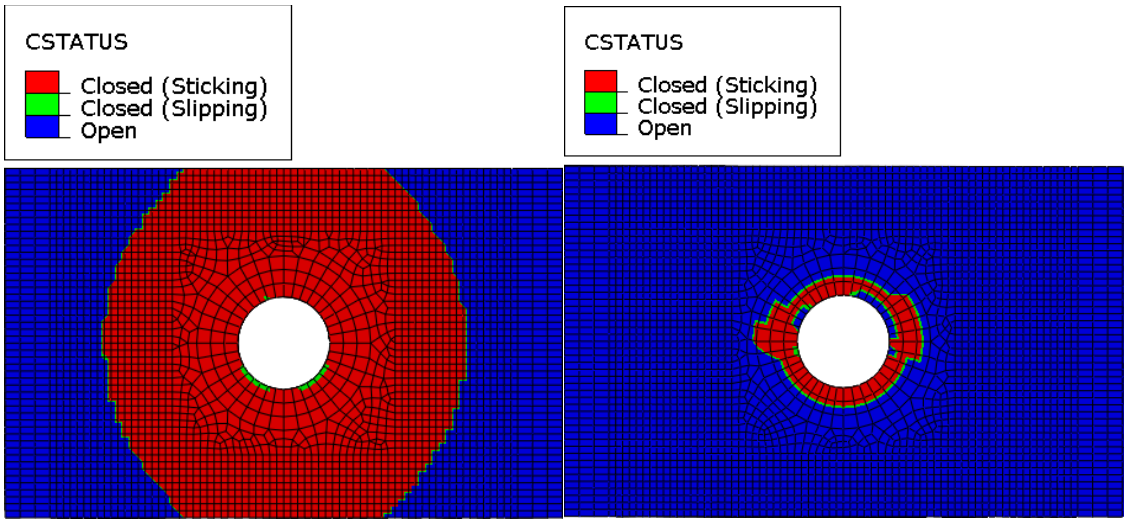

Figure 7: Abaqus CSTATUS for flat surface vs. modified surface, 21.2 Kn. Preload.

There is a dramatic difference in the area of the closed, or in contact, region of the joint. As a result, the maximum pressure in the contact (and in the micro-slip regime on the edges) will be much higher than was found for the nominally flat model. Figure 8 quantifies, the maximum contact pressure (CPRESS) of the flat interface (left) which is 17x smaller than the pressure on the modified interface (right).

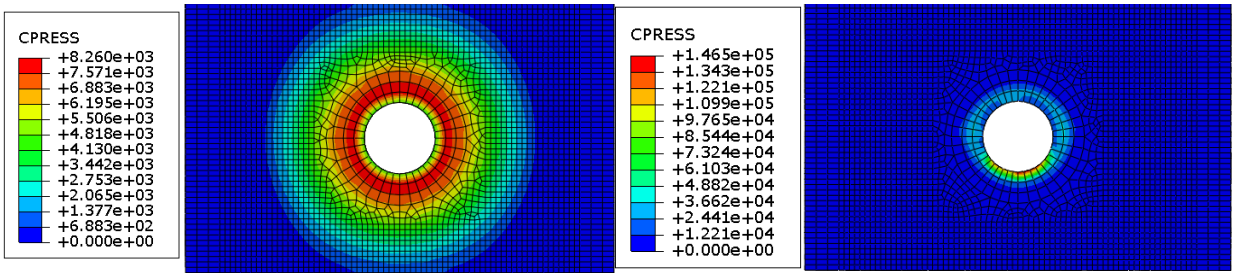

Figure 8: Abaqus CPRESS for flat surface vs. modified surface, 21.2 Kn. Preload.

In the preload study in section 4.2, very high pressures in the interface of the joint took the longest to solve. This is reinforced here as Abaqus took eight steps to solve the nonlinear preload step for the flat interface and twenty steps to solve the same

step for the modified surface. Unfortunately, because the mesh was coarsened near the hole to speed up computation for the flat-on-flat model, there is now not a sufficient mesh density to accurately resolve the microslip in the joint. A finer mesh would need to be made to study this curved interface in more depth, and thus, the model with the modified interfaces will not be explored beyond a brief preload study. The damping and frequency vs. velocity plots are compared to experimental data below.

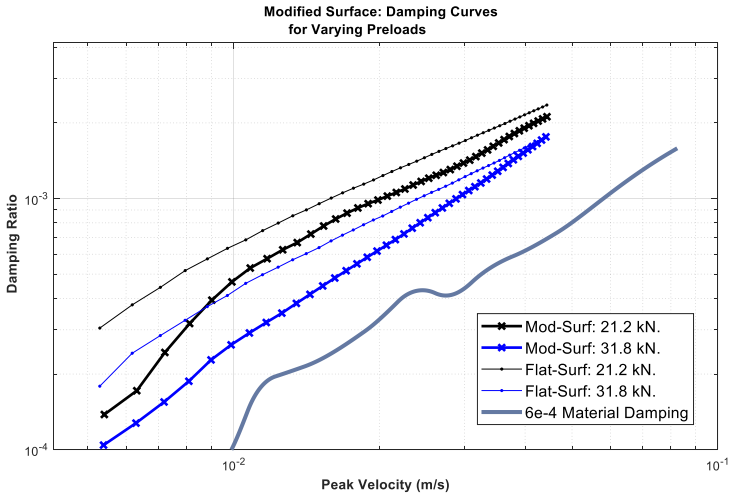

Figure 9: Damping plots for modified surface and flat surface. 1x and 1.5x nominal preloads shown against experimental data with $\zeta = 0.0006$ linear damping subtracted off.

The models with the modified surface geometry show lower damping for the same preload, which makes sense considering that the contact pressure is higher. As was the trend for the bolt preload cases in section 4.2, a higher contact pressure decreased the damping in the joint. The lack of mesh quality is apparent in the damping curve, which now deviates from power-law behavior at low amplitudes, presumably because the mesh density is insufficient to resolve the small changes that occur near the periphery of the contact.

As was the case previously, the simulations do not agree with the experimentally measured damping curves for reasonable values of the contact pressure, as shown in Figure 9. However, the mesh of the model is known to be insufficient, and so the fact that the model moves in the correct direction (towards lower damping for the higher preload) is promising.

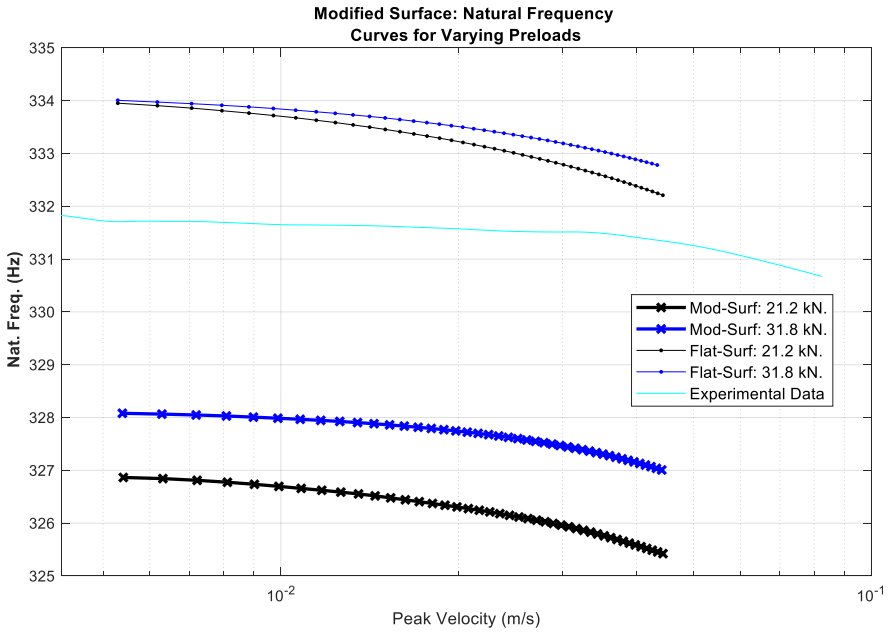

Figure 10: Natural frequency plots for modified surface and flat surface. 1x and 1.5x nominal preloads shown against experimental data.

The effect for the natural frequency is now reversed and the linear natural frequency moved closer to the experimental measurement with higher pressure. This is expected since the curved interfaces now provide a Hertzian-type contact [16] where the area of the contact increases with increasing pressure.

Comparing the natural frequency versus amplitude to the experimental data, we see that the models with a modified surface have natural frequencies that are about 4 Hz lower. Hence, the uncertainty in the interface shape may account for the shift in linear frequencies that was noted earlier; it is probable that the modulus value used is accurate but the surface geometry accounts for any discrepancies in the linear natural frequencies

One reason for the modified surfaces not bringing the model into better agreement, especially for natural frequency, could be due to poor quality measurements or the method for extrapolating a surface as described in Section 3. The biggest takeaway from these surface measurements is that implementing a realistic surface contour for a nominally flat model can produce a large effect on the dynamic behavior of the joint. It seems that it will be critical to measure the surface geometry accurately and implement that into the FEM in order to obtain better agreement in the future.

CONCLUSION AND FUTURE WORK

This paper has summarized work to date using quasi-static modal analysis (QSMA) to model nonlinearity due to micro-slip in the S4 Beam. The current model included about one million DOF, and was the smallest model that our group has been able to create to date that can capture the joints in this structure in sufficient detail while coarsening the mesh as much as possible in areas away from the joints. While it is probably possible to create a smaller model with additional effort, models of approximately this size are probably typical when seeking to describe a few joints in detail. With this model, a dynamic transient analysis would take several decades (extrapolating based on the static analysis that was performed), while with QSMA one could estimate the behavior that would be observed when the structure vibrates in one mode in 5-24 hours. While it was not demonstrated here, from the QSMA results one could reconstruct the dynamic transient response until the amplitude of vibration decayed to zero (tens of seconds in the experimental results).

This work sought to use QSMA to correlate the FEM with measurements from a real S4 Beam, in which impact testing was used to extract the nonlinear behavior of a few modes. Our initial results were qualitatively very similar to the measurements, though they over-predicted damping by about an order of magnitude. A parameter study revealed that the model could not be made to agree with the measurements unless the preload was increased far beyond the yield strength of the bolts. An investigation was performed in which the actual measured curvature of the surfaces was included in the FEM, and even though the geometry only changed by a few thousandths of an inch (about 100 microns), this had a dramatic effect on the contact pressure and on the predicted stiffness and damping of the joint. We expect that even larger differences may be observed once the FE mesh is refined to better capture the surface geometry. In retrospect, considering how stiff the structure/material is, it should have been obvious that the surface geometry would be so important.

Moving forward, the existing FE Model is also being used to compute the nonlinearity in the 6^{th} mode of vibration, which was experimentally found to exhibit even stronger nonlinearity than Mode 2, which is the mode that was studied here. New profilometry measurements will be obtained and used to create a new FE model, whose mesh will be tailored to capture the contact more accurately. It is hoped that these investigations will reveal whether it is possible to reproduce the physics (amplitude dependent damping and stiffness) that were observed in these experiments using an FE model with Coulomb friction at the interface. If this succeeds, this tool could be used to predict the effect that joints in a wide variety of structures have on the dynamics of their fundamental modes of vibration.

ACKNOWLEDGEMENTS

This material is based in part upon work supported by the National Science Foundation under Grant Number CMMI-1561810. Any opinions, findings, and conclusions or recommendations expressed in this material are those of the author(s) and do not necessarily reflect the views of the National Science Foundation.

REFERENCES

[1] E. Berger, "Friction modeling for dynamic system simulation," *Appl. Mech. Rev.*, vol. 55, no. 6, p. 535, 2002.

[2] C. J. Hartwigsen, Y. Song, D. M. McFarland, L. A. Bergman, and A. F. Vakakis, "Experimental study of non-linear effects in a typical shear lap joint configuration," *J. Sound Vib.*, vol. 277, no. 1–2, pp. 327–351, Oct. 2004.

[3] M. Groper, "Microslip and macroslip in bolted joints," *Exp. Mech.*, vol. 25, no. 2, pp. 171–174, Jun. 1985.

[4] M. Groper and J. Hemmye, "TheDissipation of Energy in High Strength Friction Grip Bolted Joints," presented at the SESA Spring Conf, ., Cleveland, OH, 1983.

[5] K. Hartwigsen, *Handbook of Lubrication, ll--Theory and Design, Part l—Frictio*. CRC Press Inc, 1983.

[6] H. Festjens, G. Chevallier, and J. Dion, "A numerical tool for the design of assembled structures under dynamic loads," *Int. J. Mech. Sci.*, vol. 75, pp. 170–177, Oct. 2013.

[7] D. D. Quinn, "Modal analysis of jointed structures," *J. Sound Vib.*, vol. 331, no. 1, pp. 81–93, Jan. 2012.

[8] D. J. Segalman, "A modal approach to modeling spatially distributed vibration energy dissipation.," SAND2010-4763, 993326, Aug. 2010.

[9] M. S. Allen, R. M. Lacayo, and M. R. Brake, "Quasi-static Modal Analysis based on Implicit Condensation for Structures with Nonlinear Joints," p. 15.

[10] D. J. Segalman, "A Four-Parameter Iwan Model for Lap-Type Joints," *J. Appl. Mech.*, vol. 72, no. 5, p. 752, 2005.

[11] B. J. Deaner, M. S. Allen, M. J. Starr, and D. J. Segalman, "Investigation of Modal Iwan Models for Structures with Bolted Joints," in *Topics in Experimental Dynamic Substructuring, Volume 2*, 2014, pp. 9–25.

[12] R. M. Lacayo and M. S. Allen, "Updating structural models containing nonlinear Iwan joints using quasi-static modal analysis," *Mech. Syst. Signal Process.*, vol. 118, pp. 133–157, Mar. 2019.

[13] E. A. Jewell, M. S. Allen, and R. Lacayo, "Predicting Damping of a Cantilever Beam With a Bolted Joint Using Quasi-Static Modal Analysis," p. V008T12A019, Aug. 2017.

[14] I. Zare, M. S. Allen, and E. Jewell, *An Enhanced Static Reduction Algorithm for Predictive Modeling of Bolted Joints*. Cham: Springer International Publishing, 2019.

[15] I. Zare and M. S. Allen, "A Block-Gauss Seidel Algorithm with Static Reduction to Predict Damping in Bolted Joints," presented at the in International Seminar on Modal Analysis (ISMA), Leuven, Belgium, 2018, p. 12.

[16] Y. J. Ahn and J. R. Barber, "Response of frictional receding contact problems to cyclic loading," *Int. J. Mech. Sci.*, vol. 50, no. 10–11, pp. 1519–1525, Oct. 2008.

[17] R. C. Flicek, D. A. Hills, J. R. Barber, and D. Dini, "Determination of the shakedown limit for large, discrete frictional systems," *Eur. J. Mech. - ASolids*, vol. 49, pp. 242–250, Jan. 2015.

[18] G. Masing and W. Mauksch, "Eigenspannungen und Verfestigung des plastisch gedehnten und gestauchten Messings," in *Wissenschaftliche Veröffentlichungen aus dem Siemens-Konzern: IV. Band. Zweites Heft*, Berlin, Heidelberg: Springer Berlin Heidelberg, 1925, pp. 244–256.

[19] A. Singh *et al.*, "Experimental Characterization of a New Benchmark Structure for Prediction of Damping Nonlinearity," in *Nonlinear Dynamics, Volume 1*, 2019, pp. 57–78.

[20] E. Jewell and M. S. Allen, "Predicting Damping of a Cantilever Beam using Finite Elements," *J. Sound Vib.*

[21] B. Lyndon, "Criteria for Preloaded Bolts," p. 38.

[22] N. Motosh, "Development of Design Charts for Bolts Preloaded up to the Plastic Range," *J. Eng. Ind.*, vol. 98, no. 3, p. 849, 1976.

[23] M. Fronk *et al.*, "Inverse Methods for Characterization of Contact Areas in Mechanical Systems," in *Nonlinear Dynamics, Volume 1*, 2019, pp. 45–56.

[24] N. M. Ames *et al.*, "Handbook on dynamics of jointed structures.," SAND2009-4164, 1028891, Jul. 2009.